

IMPROVED TEMPLATES FOR PHOTOMETRIC REDSHIFTS
OF SUBMM SOURCESL. K. HUNT¹
ANDR. MAIOLINO²

ABSTRACT

There is growing evidence that some star-forming galaxies at $z > 1$ are characterized by high efficiencies and specific star formation rates. In the local universe, these traits are shared by “active” Blue Compact Dwarf galaxies (BCDs) with compact and dense star-forming regions. The Spectral Energy Distributions (SEDs) of these BCDs are dominated by young massive star clusters, embedded in a cocoon of dust. In this Letter, we incorporate these BCD SEDs as templates for two samples of high-redshift galaxy populations selected at submm wavelengths. Because of the severe absorption of the optical light, the featureless mid-infrared spectrum, and the relatively flat radio continuum, the dusty star-cluster SEDs are good approximations to most of the submm sources in our samples. In most cases, the active BCD SEDs fit the observed photometric points better than the “standard” templates, M 82 and Arp 220, and predict photometric redshifts significantly closer to the spectroscopic ones. Our results strongly suggest that the embedded dusty star clusters in BCD galaxies are superior to other local templates such as M 82 and Arp 220 in fitting distant submm starburst galaxies.

Subject headings: galaxies: high-redshift — galaxies: starburst — submillimeter — infrared: galaxies

1. INTRODUCTION

The extension of the photometric redshift technique to the far-infrared (FIR) and radio spectral ranges has proven to be a useful tool to investigate the population of distant sub-millimeter (submm) sources (Smail et al. 1997; Barger et al. 1998; Hughes et al. 1998) which, because of heavy dust obscuration, may have optical counterparts that are too faint for a spectroscopic identification (e.g. Barger et al. 1999). This technique, first proposed by Carilli & Yun (1999), initially exploited only the radio-to-submm spectral index as a redshift indicator, and is still hotly debated because of the degeneracy between increasing redshift and decreasing dust temperature (Blain 1999; Blain et al. 2003; Aretxaga et al. 2005). Nevertheless, it has recently been extended also to other bands (Greve et al. 2004; Eales et al. 2003), including new Spitzer data (e.g. Appleton et al. 2004; Frayer et al. 2004). The templates commonly used to fit the FIR-to-radio SED of high redshift dusty galaxies are those of well studied, evolved starburst galaxies in the local universe (typically Arp220 and M82), or Active Galactic Nuclei (AGNs) (e.g. Aretxaga et al. 2003). This approach assumes that dusty starburst galaxies at high redshift are characterized by the same physical properties as local “standard” starburst galaxies.

However, there is growing evidence that some starburst galaxies at $z > 1$ are characterized by a different regime of star formation. Bauer et al. (2005) have shown that the specific star formation rate ($\text{SSFR} \equiv \text{SFR}/\text{galaxy mass}$) at $z > 1$ is significantly higher than observed in the local universe (see also Feulner et al. 2005; Greve et al. 2005). New Spitzer data reveal that a significant fraction of high-redshift sources are characterized by the ab-

sence of PAH features in their mid-IR spectra (Houck et al. 2005). Houck et al. (2005) interpret these observations as a possible indication for AGN-powered galaxies, but a lack of PAH features is also observed in extragalactic extremely compact star forming regions (Thuan et al. 1999; Houck et al. 2004; Galliano et al. 2005). Finally, many high- z submm galaxies show dust obscuration much more extreme than observed in local “standard” starburst templates (Hammer et al. 2005), and may more closely resemble highly efficient maximum-intensity starbursts (Meurer et al. 1997; Somerville et al. 2001; Greve et al. 2005).

The Blue Compact Dwarf (BCD) galaxies found in the local universe are certainly less luminous and much less massive than the submm starburst galaxies found at high redshift. They are also more metal poor, and therefore distinct from the massive “SCUBA galaxies” and Lyman-break systems which are already chemically enriched at $z \lesssim 3$ (Pettini et al. 2001; Tecza et al. 2004; Shapley et al. 2004). However, a subclass of them, “active” BCDs (Hirashita & Hunt 2004), seems to share one characteristic with the high-redshift submm population: extreme star forming modes. Active BCDs host extremely compact, very young, super star clusters, which are responsible for a very efficient SSFR, and which dominate their Spectral Energy Distributions (SEDs) (Vanzi & Sauvage 2004; Hunt et al. 2005). The intense SSFR and the compactness of the star forming regions makes the infrared SEDs of active BCDs quite different from “classical” starburst galaxies, often being broader and/or warmer, and featureless (Hunt et al. 2005). The youth of these systems tends to make the radio emission predominantly thermal rather than synchrotron (Klein et al. 1991; Hunt et al. 2005). Super star clusters in BCDs can also be heavily embedded in

¹ INAF–Istituto di Radioastronomia, Largo E. Fermi 5, 50125 Firenze, Italy; hunt@arcetri.astro.it

² INAF–Osservatorio Astrofisico di Arcetri, Largo E. Fermi 5, 50125 Firenze, Italy; maiolino@arcetri.astro.it

dust, which makes the stellar and nebular radiation heavily absorbed even in the near-IR (Hunt et al. 2001). These extreme properties of BCDs suggest that they may represent a scaled down version of the extreme starburst galaxies at high redshift. In particular, BCDs could provide better templates for the SEDs of distant starburst galaxies, thus enabling more accurate photometric redshifts.

In this Letter we test this hypothesis by comparing the SEDs of local BCDs (Hunt et al. 2005) with the photometric measurements of high redshift submm galaxies having secure spectroscopic identifications and redshifts. We show that BCD templates generally provide a better match to the SEDs of submm/SCUBA galaxies and improve significantly the accuracy of photometric redshifts.

2. THE BCD SED TEMPLATES

The SEDs from $5\ \mu\text{m}$ to 20 cm of low-metallicity “active” BCDs are well modelled by dusty massive star clusters (Hunt et al. 2005). We have taken three cases from Hunt et al. (2005): NGC 5253, II Zw 40, and SBS0335–052, which are characterized by different amounts of dust extinction: $A_V = 10, 20,$ and $30\ \text{mag}$, respectively. Because the SED of SBS0335–052 is very unusual, peaking at $\sim 30\ \mu\text{m}$, we have also included another best-fit model for II Zw 40 with $A_V = 30\ \text{mag}$. Also for II Zw 40, we adopted two possible values for the radio slope: pure thermal $\alpha = -0.1$, and supernova-like $\alpha = -0.5$, both of which are consistent with the data.

Rather than the entire observed BCD SED, we adopt here only the dusty star cluster SED, as given by Hunt et al. (2005), which are based on *DUSTY* (Ivezić & Elitzur 1997) models. Because of the large optical depths, the rest-wavelength optical bands in these SED templates are highly reddened and absorbed. The observed optical SEDs of BCDs are not well modelled by the dusty clusters, because the optical light arises from regions outside of the clusters, or at least from regions which are not subject to their high extinction. We do not consider such emission in our SED templates.

The BCDs which we are using as SEDs are generally metal poor. However, the ISM metallicity determines, at least in part, *only* the dust content (e.g., Edmunds 2001), so that it becomes a scaling factor, rather than a shaping factor in the SED. Observationally, these star-cluster SEDs are applicable to a wide range of metal abundances, from highly sub-solar (SBS 0335–052, $\sim 2.5\% Z_\odot$) to \sim solar (He 2–10) (Hunt et al. 2005). Hence, the SEDs we are using to model high-z sources are essentially independent of metallicity.

3. BCDS VERSUS SUBMM GALAXIES WITH SPITZER DATA

A few submm sources (e.g., Smail et al. 1997; Barger et al. 1998; Hughes et al. 1998) have recently been observed with Spitzer (Egami et al. 2004; Frayer et al. 2004; Ivison et al. 2004; Higdon et al. 2004). Such new data allow a more detailed analysis of the IR-to-radio SED of these distant starburst galaxies than previously possible. Among the submm galaxies observed with Spitzer we have selected those with secure spectroscopic redshifts³. These six sources and their basic properties are listed in Table

1. None of them seem to host powerful AGN, at least according to their optical spectra. Due to the limited space available in this Letter, the photometric points for only three of the six sources are plotted in Fig. 1.

We have fit the observed SEDs with the six templates described in §2. The “fit” is a scaling normalization to minimize residuals, and a calculation of the remaining (logarithmic) rms deviations. For comparison with the templates adopted in the past, we also fit the SEDs with the spectrophotometric models of M 82 and Arp 220 given by Bressan et al. (2002). In total, we consider eight templates: six variations of BCD star clusters, M 82, and Arp 220. In Fig. 1 we show examples of the various templates redshifted to the spectroscopic redshift and scaled to best fit the photometric measurements. In Table 1 we give the rms residuals for the best-fit template evaluated at the spectroscopic redshift. In four of the six cases, the BCD templates fit significantly better the observed photometric points than either M 82 or Arp 220.

We have also tested the capability of each template to reproduce the spectroscopic redshift through the photometric redshift technique. First, the SEDs were convolved with the Spitzer filters. Then, by finding the minimum of χ^2 residuals as a function of redshift for the various templates, we derived the photometric redshift for each source. Table 1 reports the photometric redshifts obtained for each template. It is impressive that the BCD templates *always* provide a photometric redshift closer to the actual, spectroscopic redshift than obtained with M 82 or Arp 220.

The smallest average $z_{\text{phot}} - z_{\text{spec}}$ and standard deviation is obtained with the II Zw 40 model having $A_V = 20\ \text{mag}$ and a thermal radio spectrum. If we were to calculate photometric redshifts of the objects in this sample using this SED, we would obtain a mean and standard deviation of $\langle z_{\text{phot}} - z_{\text{spec}} \rangle = 0.02 \pm 0.50$. If we use SBS 0335–052 ($A_V = 30\ \text{mag}$ $\alpha = -0.3$), we would obtain a mean and standard deviation of $\langle z_{\text{phot}} - z_{\text{spec}} \rangle = 0.17 \pm 0.61$. Were we to use Arp 220 (M 82), we would obtain results inferior to both of these with large means and significantly larger scatters: $\langle z_{\text{phot}} - z_{\text{spec}} \rangle = 0.8(2.5) \pm 1.0(1.5)$.

The reason that BCD SEDs better match the observed SEDs in these high-z submm galaxies with Spitzer IRAC+MIPS data is a combination of some or all of the following effects: 1) the $\lesssim 5\ \mu\text{m}$ region (stellar light) is much more absorbed in some BCDs than in the M 82 and Arp 220 templates; 2) all (active, see Hunt et al. 2005) BCDs are featureless in the mid-IR; 3) the infrared bump is broader in some BCD SEDs; 4) the flatter thermal radio continuum of some BCDs better matches the radio observations in some sources.

4. BCDS VERSUS SUBMM GALAXIES WITH ONLY RADIO DATA

Thanks to the recent spectroscopic surveys of submm sources with radio counterparts, large samples of submm sources with secure spectroscopic redshifts are now available (e.g. Chapman et al. 2005). For most of these sources Spitzer data are not yet published, making unfeasible a detailed analysis such as the one performed in the previous section. However, we can test the photometric redshift technique by exploiting the $850\ \mu\text{m}$ and radio data, as was

³ A seventh source would also be available, but it is lensed and therefore more complex to interpret.

done for most submm sources in the past.

We have compiled a list of all SCUBA sources with spectroscopic redshifts (Chapman et al. 2002, 2005), discarding those lensed and with multiple counterparts to avoid complications that may arise in the interpretation of the SED in these cases. We have also discarded sources whose spectra show clear signatures of an AGN, since in this Letter we focus on the interpretation of the SEDs due to star formation alone. These selection criteria resulted in a sample of 40 sources, which are listed in Table 2.

For each source we estimated the submm-to-radio photometric redshift by using both the BCD templates and the ‘classical’ templates M82 and Arp220, as discussed in the previous section. We found that in 63% (25/40) of the cases, BCD templates provide a photometric redshift that is closer to the spectroscopic one than with M82 or Arp220. Moreover, the mean difference $\langle z_{\text{phot}} - z_{\text{spec}} \rangle$ averaged over the sample is significantly reduced for the BCD templates (~ 0.1 for NGC 5253), relative to M82 (~ 0.5) or Arp220 (~ 0.8). If we analyze all 62 objects, including those with known AGN/QSO emission, we obtain a similar result: in 61% (38/62) of the cases, BCD templates provide a better photometric redshift than either M82 or Arp220. These results are summarized in Table 2, while Fig. 2 shows the distribution of $z_{\text{phot}} - z_{\text{spec}}$ for different templates. It is clear that the BCD template for NGC 5253 gives a distribution much more peaked around zero.

For this sample of 40 objects, whose SEDs comprise only submm and radio fluxes, the SED which best predicts z_{phot} is NGC 5253, with an $A_V = 10$ mag and a thermal

radio spectrum. More than 60% of the radio-identified submm sources are better fit with a flatter radio spectrum ($-0.1 \leq \alpha \leq -0.3$) than with the usual steeper spectrum $\alpha \approx -0.7$, observed in virtually all evolved starbursts (Condon 1992).

5. CONCLUSIONS

‘Active’ BCDs may be characterized by star formation modes similar to those in high- z starburst galaxies, specifically for the efficiency and compactness of the star formation. We have compared the observed SEDs of spectroscopically identified submm galaxies with BCD SED templates, for both a small sample of submm galaxies with sensitive Spitzer observations, and a larger sample of submm galaxies with only radio (and submm) data. In most cases we find that BCD galaxies match the SED observed in distant submm galaxies better than the more widely adopted templates of ‘standard’ starbursts (M82 and Arp220). If the BCD templates are used for the photometric redshift technique, then the inferred z_{phot} are significantly closer to the actual spectroscopic redshifts than what is inferred by using the templates of M82 or Arp220. Our results strongly suggest that the dusty embedded star clusters in BCD galaxies provide superior templates to derive photometric redshift of distant submm, starburst galaxies which may be too faint to be identified spectroscopically.

We are grateful to Simone Bianchi, Reinhard Genzel, Linda Tacconi for insight and critical comments.

REFERENCES

- Appleton, P. N., et al. 2004, ApJS, 154, 147
 Aretxaga, I., Hughes, D. H., Chapin, E. L., Gaztañaga, E., Dunlop, J. S., & Ivison, R. J. 2003, MNRAS, 342, 759
 Aretxaga, I., Hughes, D. H., & Dunlop, J. S. 2005, MNRAS, 358, 1240
 Barger, A. J., Cowie, L. L., Sanders, D. B., Fulton, E., Taniguchi, Y., Sato, Y., Kawara, K., & Okuda, H. 1998, Nature, 394, 248
 Barger, A. J., Cowie, L. L., Smail, I., Ivison, R. J., Blain, A. W., & Kneib, J.-P. 1999, AJ, 117, 2656
 Bauer, A. E., Drory, N., Hill, G. J., & Feulner, G. 2005, ApJ, 621, L89
 Blain, A. W. 1999, MNRAS, 309, 955
 Blain, A. W., Barnard, V. E., & Chapman, S. C. 2003, MNRAS, 338, 733
 Bressan, A., Silva, L., & Granato, G. L. 2002, A&A, 392, 377
 Carilli, C. L., & Yun, M. S. 1999, ApJ, 513, L13
 Chapman, S. C., Smail, I., Ivison, R. J., Helou, G., Dale, D. A., & Lagache, G. 2002, ApJ, 573, 66
 Chapman, S. C., Blain, A. W., Smail, I., & Ivison, R. J. 2005, ApJ, 622, 772
 Condon, J. J. 1992, ARA&A, 30, 575
 Eales, S., Bertoldi, F., Ivison, R., Carilli, C., Dunne, L., & Owen, F. 2003, MNRAS, 344, 169
 Edmunds, M. G. 2001, MNRAS, 328, 223
 Egami, E., et al. 2004, ApJS, 154, 130
 Feulner, G., Goranova, Y., Drory, N., Hopp, U., & Bender, R. 2005, MNRAS, 358, L1
 Frayer, D. T., et al. 2004, ApJS, 154, 137
 Galliano, F., Madden, S.C., Jones, A.P., Wilson, C.D., Bernard, J.-P. 2005, A&A, in press (*astro-ph/0501632*)
 Greve, T. R., Ivison, R. J., Bertoldi, F., Stevens, J. A., Dunlop, J. S., Lutz, D., & Carilli, C. L. 2004, MNRAS, 354, 779
 Greve, T. R. et al. 2005, MNRAS, in press (*astro-ph/0503055*)
 Hammer, F., Flores, H., Elbaz, D., Zheng, X. Z., Liang, Y. C., & Cesarsky, C. 2005, A&A, 430, 115
 Higdon, S. J. U., et al. 2004, ApJS, 154, 174
 Hirashita, H. & Hunt, L. K. 2004, A&A, 421, 555
 Houck et al. 2005, ApJ, in press (*astro-ph/0502216*)
 Houck, J. R., et al. 2004, ApJS, 154, 211
 Hughes, D. H., et al. 1998, Nature, 394, 241
 Hunt, L.K., Bianchi, S., & Maiolino, R. 2005, A&A, in press (*astro-ph/0501188*)
 Hunt, L. K., Vanzì, L., & Thuan, T. X. 2001, A&A, 377, 66
 Ivezić, Z. & Elitzur, M. 1997, MNRAS, 287, 799
 Ivison, R. J., et al. 2002, MNRAS, 337, 1
 Ivison, R. J., et al. 2004, ApJS, 154, 124
 Klein, U., Weiland, H., & Brinks, E. 1991, A&A, 246, 323
 Meurer, G. R., Heckman, T. M., Lehnert, M. D., Leitherer, C., & Lowenthal, J. 1997, AJ, 114, 54
 Pettini, M., Shapley, A. E., Steidel, C. C., Cuby, J., Dickinson, M., Moorwood, A. F. M., Adelberger, K. L., & Giavalisco, M. 2001, ApJ, 554, 981
 Scott, S. E., et al. 2002, MNRAS, 331, 817
 Shapley, A. E., Erb, D. K., Pettini, M., Steidel, C. C., & Adelberger, K. L. 2004, ApJ, 612, 108
 Somerville, R. S., Primack, J. R., & Faber, S. M. 2001, MNRAS, 320, 504
 Smail, I., Ivison, R. J., & Blain, A. W. 1997, ApJ, 490, L5
 Tecza, M., et al. 2004, ApJ, 605, L109
 Thuan, T. X., Sauvage, M., & Madden, S. 1999, ApJ, 516, 783
 Vanzì, L., & Sauvage, M. 2004, A&A, 415, 509

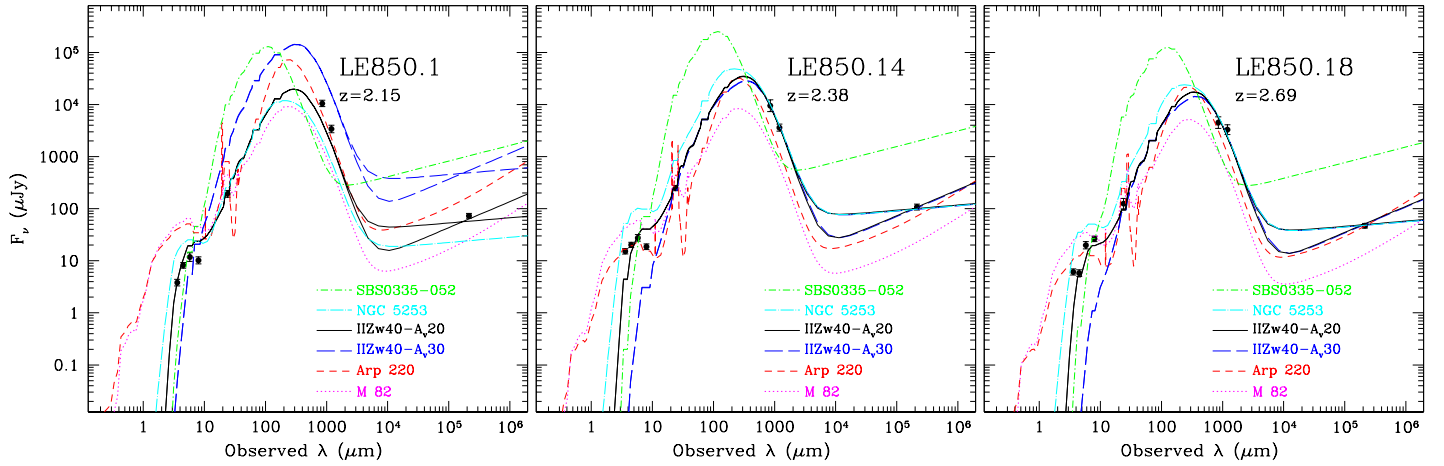


FIG. 1.— SEDs of radio-identified submm sources (Scott et al. 2002; Ivison et al. 2002; Egami et al. 2004; Ivison et al. 2004), with various starburst templates normalized to the data (see text). The best-fit BCD SED templates are II Zw 40 ($A_V = 20$ mag, $\alpha = -0.5$) for LE 850.1 and II Zw 40 ($A_V = 20$ mag, $\alpha = -0.1$) for LE 850.8 and LE 850.14.

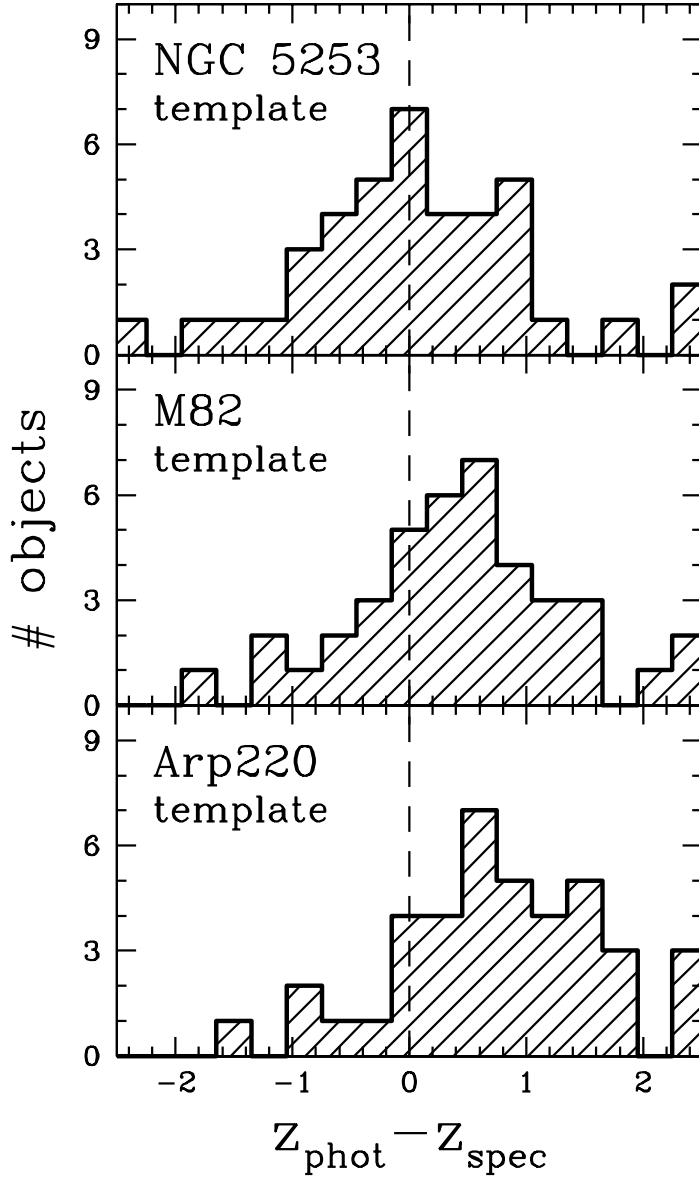


FIG. 2.— Histograms of the $z_{\text{phot}} - z_{\text{spec}}$ best-fit BCD template, NGC 5253, and the two “standard” templates, M 82 and Arp 220. The spread is similar for all three templates, but the zero mean of NGC 5253 is evident.

TABLE 1
 PHOTOMETRIC REDSHIFTS $z_{\text{phot}} - z_{\text{spec}}$ AND RESIDUALS FOR SUBMM-SELECTED SCUBA SOURCES WITH VLA AND SPITZER DATA

Source	$z_{\text{spec}}^{\text{a}}$	$\langle \text{Res.} \rangle^{\text{b}}$	II Zw 40				NGC 5253	SBS 0335-052	M 82	Arp 220
			$\alpha = -0.5$		$\alpha = -0.1$		$\alpha = -0.1$	$\alpha = -0.3$		
			$A_V = 30$	$A_V = 20$	$A_V = 30$	$A_V = 20$	$A_V = 10$	$A_V = 30$	(7)	(8)
			(1)	(2)	(3)	(4)	(5)	(6)		
CFRS14.1157	1.15	0.15 (5)	-0.75	-0.75	-0.65	-0.65	-0.35	0.95	-0.35	-0.95
Fraye.199	1.06	0.32 (8)	-0.46	0.64	-0.36	0.64	1.64	0.34	2.14	1.64
LE850.1	2.15	0.36 (2)	-0.95	0.45	-0.95	0.45	1.65	0.25	3.85	1.05
LE850.8	0.85	0.44 (4)	-0.35	0.35	-0.35	0.25	0.85	0.55	2.35	1.85
LE850.14	2.40	0.23 (4)	-1.40	-0.30	-1.40	-0.30	0.80	-0.40	3.40	0.80
LE850.18	2.69	0.25 (8)	-1.69	-0.29	-1.69	-0.29	0.81	-0.69	3.31	0.51
$\langle dz \rangle$			-0.93	0.02	-0.90	0.02	0.90	0.17	2.45	0.82
Std.dev.			0.53	0.54	0.55	0.50	0.73	0.61	1.52	1.00

^a z_{spec} from Higdon et al. (2004); Frayer et al. (2004); Chapman et al. (2005); Ivison et al. (2004); Chapman et al. (2005); Egami et al. (2004).

^b Lowest residuals for $z=z_{\text{spec}}$, obtained with the template in parentheses.

TABLE 2
PHOTOMETRIC REDSHIFTS $z_{\text{phot}} - z_{\text{spec}}$ AND RESIDUALS FOR SUBMM-SELECTED SCUBA SOURCES WITH VLA DATA ONLY

Source ^a	z_{spec} ^a	$\langle \text{Res.} \rangle^b$	II Zw 40				NGC 5253	SBS 0335-052	M 82	Arp 220
			$\alpha = -0.5$		$\alpha = -0.1$		$\alpha = -0.1$	$\alpha = -0.3$		
			$A_V = 30$	$A_V = 20$	$A_V = 30$	$A_V = 20$	$A_V = 10$	$A_V = 30$	(7)	(8)
			(1)	(2)	(3)	(4)	(5)	(6)		
FN1-40	0.45	3	0.35	0.45	0.25	0.35	0.35	4.45	0.65	1.05
FN1-64	0.91	1	-0.01	0.09	-0.11	-0.01	0.09	4.39	0.29	0.59
030231.81+001031.3	1.32	3	1.28	1.38	1.18	1.28	1.18	5.68	1.58	1.88
030236.15+000817.1	2.44	7	-0.23	-0.14	-0.34	-0.23	-0.34	4.57	0.07	0.47
030244.82+000632.3	0.18	3	1.22	1.32	1.02	1.12	1.02	6.82	1.42	1.82
105151.69+572636.0	1.15	3	0.65	0.75	0.55	0.55	0.55	5.85	0.95	1.35
$\langle dz \rangle$			0.25	0.26	0.14	0.19	0.10	4.89	0.47	0.79
Std.dev.			1.13	1.05	1.20	1.18	1.12	0.83	1.05	1.02

complete version of this table is in the electronic edition of the Journal. The printed edition contains only a sample.]

^aSources and z_{spec} from Chapman et al. (2002, 2005).

^b Lowest residuals for $z=z_{\text{spec}}$ obtained with this template.

[The